Supplementary Information for

Electrochemical Upgrading of Biomass-derived 5-Hydroxymethylfurfural and Furfural over Oxygen Vacancy-rich NiCoMn-Layered Double Hydroxides Nanosheets

Biying Liu,‡[a] Shaojun Xu,‡[b, c] Man Zhang,[a] Xin Li,[a] Donato Decarolis,[b, c] Yuqian Liu,[a] Yuchen Wang,[a] Emma K. Gibson,[c, d] C. Richard A. Catlow[b, c, d] and Kai Yan*[a]

[a.] *Guangdong Provincial Key Laboratory of Environmental Pollution Control and Remediation Technology, School of Environmental Science and Engineering, Sun Yat-sen University, Guangzhou 510275, China.*

[b.] *School of Chemistry, Cardiff University, Main Building, Park Place, Cardiff, CF10 3AT, United Kingdom.*

[c.] *UK Catalysis Hub, Research Complex at Harwell, Rutherford Appleton Laboratory, Harwell, OX11 0FA, United Kingdom.*

[d.] *School of Chemistry, Joseph Black Building, University of Glasgow, Glasgow G12 8QQ, United Kingdom*

[e.] *Department of Chemistry, University College London, 20 Gordon Street, London, WC1H 0AJ, United Kingdom*

‡ These Authors contribute equally to this work.

* Corresponding author E-mail: yank9@mail.sysu.edu.cn.

Characterization techniques

To analyze the qualitative phase of different ratios of NiCoMn-LDHs/NF, X-ray diffraction (XRD), D/max-2200vpc (RIGAKU, Japan), was applied under the condition of 40 kV and 40 mA with a Cu Kα radiation, scan rate at 10° min^{-1} and 2-Theta degree ranging from 10° to 80°.

Electron paramagnetic resonance (EPR, Burker A300) was conducted to determine the vacancies on the surface of the powder catalyst.

Raman spectra were measured by Raman spectroscopy (DXR2 XI) with a 532 nm laser excitation.

X-ray photoelectron spectroscopy (XPS, Nexsa) was investigated with monochromatic Al Kα X-ray as the excitation source and a pass energy of 40 eV to find the changes of valence on NiCoMn-LDHs/NF after oxidation reaction.

Atomic Force Microscope (AFM, NanoManVS) was operated to decide the thickness of the powder catalysts.

Scanning electron microscopy (SEM, Quanta 400 FEG) was used to observe the morphology of NiCoMn-LDHs grown on Ni foam (NF).

The microstructure of the powder NiCoMn-LDHs were characterized by and Transmission electron microscope (TEM, FEI Tecnai G2 F20).

Elemental analysis for all prepared catalysts was tested using Thermo iCap 6300 inductively coupled plasma optical emission spectroscopy (ICP-OES).

The X-ray absorption fine structure (XAFS) measurements were performed in B18 beamline at Diamond Light Source at the Mn, Co and Ni K edge (6.53, 7.7 and 7.85 keV, respectively) in transmission mode using a Si (111) monochromator for energy selection, using ion chambers to detect X-rays. The sample, mixed with cellulose, was formed into pellets which were then loaded in the beamline where XAFS measurement were performed. Data processing and analysis were done using Athena and Artemis software from the Demeter IFEFFIT package. The FEFF6 code was used to construct theoretical EXAFS signals using the quick first-shell feature of Artemis. For Mn K-edge a Mn-O and a Mn-Mn path were chosen, at 2.1 Å and 2.9 Å respectively. For Co K-edge a Co-O and a Co-Co path were chosen, at 2.1 Å and 3.3 Å respectively. For Ni K-edge a Ni-O and a Ni-Ni were chosen, at 2.1 Å and 3.1 Å. The k-range used for the fitting 3–12 Å−1 and the R-range from 1 to 3.55 Å. The path degeneracy was allowed to vary in the fit in order to account for the size effects that cause surface atoms to be less coordinated than those in the particle interior. The amplitude reduction factor (S20) was fixed at 0.78 for all measurements.

Table S1. Detailed ratios of mixed metal solution when preparing NiCoMn-LDHs.

LDHs	**$V_{0.5\ M\ Ni^{2+}\ (aq.)}$ / mL**	**$V_{0.5\ M\ Co^{2+}\ (aq.)}$ / mL**	**$V_{0.5\ M\ Mn^{2+}\ (aq.)}$ / mL**	**pH**
NiCoMn(1:1)-LDHs	0.750	0.750	1.500	8.5
NiCoMn(2:1)-LDHs	1.000	1.000	1.000	8.5
NiCoMn(3:1)-LDHs	1.125	1.125	0.750	8.5

Table S2. Information of chemical reagents.

Chemical reagents	Specifications	Manufacturer
$Ni(NO_3)_2{\cdot}4H_2O$	98+%	Alfa Aesar
$Co(NO_3)_2{\cdot}4H_2O$	98%	Alfa Aesar
$Mn(NO_3)_2{\cdot}4H_2O$	99.999%	Alfa Aesar
NaOH	97%	Macklin
Na_2CO_3	GR 99.9%	Macklin
$C_6H_6O_3$	98+%	Alfa Aesar
HCl	AR	Guangzhou Chemical Reagent Factory
CH_3COCH_3	AR	Chengdu KESHI Company
H_2SO_4	AR	Guangzhou Chemical Reagent Factory
CH_3OH	HP	Aladdin
$HCOONH_4$	HP	Aladdin
$C_6H_4O_5$	98%	Alfa Aesar
$C_6H_4O_3$	98%	Alfa Aesar
$C_6H_6O_4$	98%	Alfa Aesar
$C_5H_4O_2$	99%	Macklin
$C_5H_4O_3$	99%	Macklin

Table S3. Effect of different Mn levels on structural parameters of NiCoMn-LDH/NF.

LDHs	**$d_{(003)}$ (Å)**	**$d_{(110)}$ (Å)**	***c* (Å)**	***a* (Å)**	**$D_{(003)}$ (nm)**
NiCoMn(1:1)-LDHs/NF	7.756	1.466	23.269	2.932	20.726
NiCoMn(2:1)-LDHs/NF	7.455	1.452	22.366	2.903	19.968
NiCoMn(3:1)-LDHs/NF	7.571	1.451	22.712	2.902	21.627

Table S4. The weight (wt. %) and the molar mass ratio of metals.

	wt. %					
	Ni	Co	Mn	C	H	N
NiCoMn(1:1)-LDHs	15.31	19.22	22.42	0.72	1.14	0.31
NiCoMn(2:1)-LDHs	15.31	13.84	8.18	0.5	1.08	<0.3

Table S5. Local structure parameters around Ni estimated by EXAFS analysis.

$CN_{Ni\text{-}O}$[a]	$R_{Ni\text{-}O}$ (Å) [b]	$\sigma^2_{Ni\text{-}O}$[c]	$CN_{Ni\text{-}Ni}$	$R_{Ni\text{-}Ni}$ (Å)	$\sigma^2_{Ni\text{-}Ni}$	ΔE	R_{factor}
7.9 ± 0.5	2.043 ± 0.005	0.007 ± 0.0009	8 ± 1	3.06 ± 0.005	0.01 ± 0.001	-6.3 ± 0.5	0.006

[a] CN = coordination number

[b] R = distance between absorber and backscattering atoms

[c] σ^2= Debye-Waller factor

Table S6. Local structure parameters around Co estimated by EXAFS analysis.

$CN_{Co\text{-}O}$	$R_{Co\text{-}O}$ (Å)	$\sigma^2_{Co\text{-}O}$	$CN_{Co\text{-}Co}$	$R_{Co\text{-}Co}$ (Å)	$\sigma^2_{Co\text{-}Co}$	ΔE	R_{factor}
5 ± 1	1.9 ± 0.01	0.008 ± 0.002	5 ± 1	3.39 ± 0.02	0.006 ± 0.002	-12 ± 2	0.04

Table S7. Local structure parameters around Mn estimated by EXAFS analysis.

$CN_{Mn\text{-}O}$	$R_{Mn\text{-}O}$ (Å)	$\sigma^2_{Mn\text{-}O}$	$CN_{Mn\text{-}Mn}$	$R_{Mn\text{-}Mn}$ (Å)	$\sigma^2_{Mn\text{-}Mn}$	ΔE	R_{factor}
4.2 ± 0.4	1.914 ± 0.008	0.004 ± 0.001	9 ± 3	3.02 ± 0.02	0.022 ± 0.006	-3 ± 1	0.02

Table S8. Comparison of oxidation of HMF and furfural catalyzed by different anodic catalysts and under different conditions in alkaline electrolytes from previous reports.

Electrode	Electrolytes	Reaction condition	Conversion (%)	Yield (%)	Ref.
NiFe-LDHs	10 mM HMF	Applied potential of 1.23 $V_{RHE;}$ reaction time 10 h; room temperature	99.0	98.0	1
NiCoFe-LDHs	10 mM HMF	Applied potential of 1.52 V_{RHE}; reaction time 60 min; temperature = 55 ^{o}C	95.5	81.1 (Selective of 84.9%)	2
NiOOH	5 mM HMF	Applied potential of 1.47 $V_{RHE;}$ reaction time 4.7 h; room temperature	99.8	96.0%	3
CoOOH	5 mM HMF	Applied potential of 1.62 $V_{RHE;}$ reaction time 4.6 h; room temperature	87.5	25.6	3
FeOOH	5 mM HMF	Applied potential of 1.71 $V_{RHE;}$ reaction time 2.3 h; room temperature	16.0	1.59	3
$NiCo_2O_4$	5 mM HMF	Applied potential of 1.50 V_{RHE}; charge passed of 34.75 C; room temperature	99.63	90.5 (Selective of 90.8%)	4

CoNW/NF	100 mM HMF	Applied potential of 1.72 V_{RHE}; reaction time 5.73 h; room temperature	100	96.8	5
NiGF	10% w/w furfural	$I_{applied\ current}/I_{theoretical\ current}$ = 1.3; flow rate 2.5 mL min^{-1}	87	83	6
Au	35 mM furfural	Applied potential of 0.15 $V_{SCE;}$ reaction time 13 h; room temperature	56	53.2 (Selective of 95%)	7
Ni	50 mM furfural	Applied current density of 0.8 mA cm^{-2}; reaction time ~200 min; room temperature	Not mentioned	80	7
NiCoMn-LDHs/NF	1 mM HMF	Applied potential of 1.5 $V_{RHE;}$ reaction time 150 min; temperature = 35 ^{o}C	100	91.7	This work
NiCoMn-LDHs/NF	1 mM furfural	Applied potential of 1.5 $V_{RHE;}$ reaction time 150 min; temperature = 35 ^{o}C	96.8	92.4	This work

Table S9. The conversion of 1 mM HMF and furfural and the yield of FDCA and FurAc in different temperature (25 ^{o}C, 35 ^{o}C, 45 ^{o}C and 55 ^{o}C) by using NiCoMn(2:1)-LDHs in 150 min.

Temperature	25 ^{o}C	35 ^{o}C	45 ^{o}C	55 ^{o}C
HMF conversion	94.7	100	100	100
FDCA yield	72.9	91.7	42.3	16.3
Furfural conversion	96.5	96.8	99.9	100
FurAc yield	89.1	92.4	47.1	33.9

Table S10. The conversion of different concentration of HMF and furfural (1 mM, 5 mM, 10 mM and 20 mM) and the yield of FDCA and FurAc at the temperature of 35 ^{o}C by using NiCoMn(2:1)-LDHs in 90 min.

Reactant concentration	1 mM	5 mM	10 mM	20 mM
HMF conversion	100	100	41.5	31.4
FDCA yield	81.4	31.2	9.5	7.0
Furfural conversion	94.3	83.7	80.0	75.6
FurAc yield	88.0	61.3	54.8	48.2

Table S11. The conversion of 1 mM HMF and furfural and the yield of FDCA and FurAc at temperature of 35 ^{o}C by using NiCoMn(1:1)-LDHs/NF, NiCoMn(2:1)-LDHs/NF and NiCoMn(3:1)-LDHs/NF in 150 min.

Types of LDHs	**1:1**	**2:1**	**3:1**
HMF conversion	100	100	100
FDCA yield	60.2	91.7	83.6
Furfural conversion	98.6	96.8	100
FurAc yield	65.8	92.4	76.0

Table S12. The main binding energy values of Ni 2p, Co 2p and Mn 2p spectra.

Binding energy (eV)	**Before reaction**	**After oxidation of HMF**	**After oxidation of furfural**
Ni $2p_{3/2}$	Ni^{2+} 855.3, Ni^{3+} 857.1	Ni^{2+} 855.3, Ni^{3+} 857.2	Ni^{2+} 855.4, Ni^{3+} 857.2
Ni $2p_{1/2}$	Ni^{2+} 873.0, Ni^{3+} 874.7	Ni^{2+} 873.2, Ni^{3+} 874.9	Ni^{2+} 873.1, Ni^{3+} 875.0
Co $2p_{3/2}$	780.7	780.9	780.9
Co $2p_{1/2}$	796.3	796.6	796.6
Mn $2p_{3/2}$	Mn^{3+} 641.9, Mn^{2+} 643.6	Mn^{3+} 642.0, Mn^{2+} 645.6	Mn^{3+} 642.0, Mn^{2+} 645.6
Mn $2p_{1/2}$	654.0	654.1	654.1

Nernst equation

$$E_{RHE} = E_{Ag|AgCl}^{\theta} + 0.059\ pH + E_{Ag|AgCl}$$

In the equation, E_{RHE} represents the potential of RHE, $E_{Ag|AgCl}^{\theta}$ illustrates the theoretical potential of 0.197 V, pH is from the aqueous 1.0 M NaOH with or without biomass electrolyte and $E_{Ag|AgCl}$ is the measurement of potential relative to reference electrode tested by the electrochemical workstation.

Debye-Scherrer equation

$$D = \frac{0.94\ \lambda}{\beta\ cos\theta}$$

In the equation, D is the average particle diameter (nm); λ is the copper wavelength (0.154056 nm); β is the half-width at half maxima (FWHM) of the most intense diffraction peak (rad); and θ is the Bragg diffraction angle (deg).

Turnover frequency (TOF) calculation

$$TOF_{OER} = \frac{j \times A}{4 \times F \times m}$$

$$TOF_{HMF} = \frac{j \times A}{6 \times F \times m}$$

$$TOF_{Fur} = \frac{j \times A}{4 \times F \times m}$$

In the equation, j is the current density at different overpotential (mA cm^{-2}); A is the area of the electrode (cm^2); F is the faraday constant (96,485 C mol^{-1}); and m is the number of moles of active materials that are deposited onto the electrodes (mol).

Mass activity calculation

$$Mass\ activity = \frac{j}{Q}$$

In the equation, j is the current density at different overpotential (mA cm^{-2}); Q is the mass of active materials that are deposited onto the electrodes (mg).

Faradaic efficiency calculation

$$Faradaic\ efficiency_{HMF} = \frac{6FN_{FDCA}}{Q}$$

$$Faradaic\ efficiency_{Fur} = \frac{4FN_{FurAc}}{Q}$$

In the equation, F is the constant of 96485 C mol^{-1}; N_{FDCA} and N_{FurAc} is the mol of FDCA or FurAc formed (mol); Q is the passed charge (C).

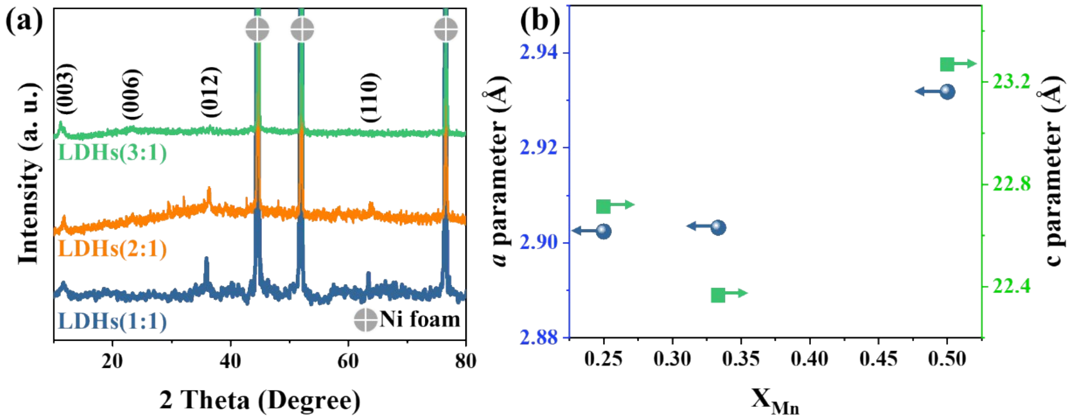

Figure S1. The crystal structure analysis. (a) XRD patterns of NiCoMn-LDHs/NF with different ratios. (b) Dependence of *a* and *c* parameters with the content of Mn (X_{Mn}).

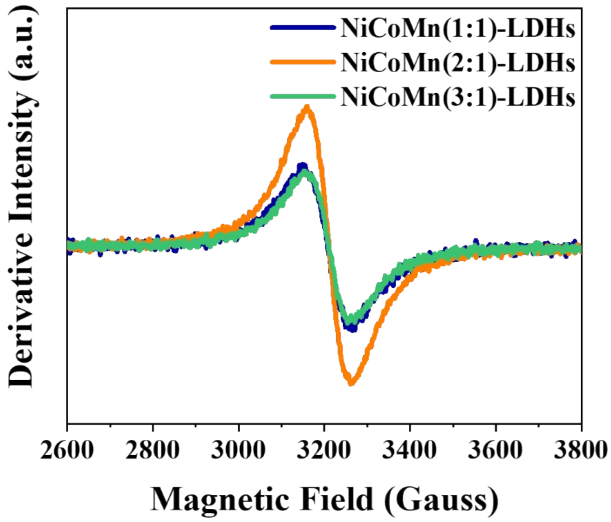

Figure S2. EPR spectra of NiCoMn(1:1)-LDHs, NiCoMn(2:1)-LDHs and NiCoMn(3:1)-LDHs.

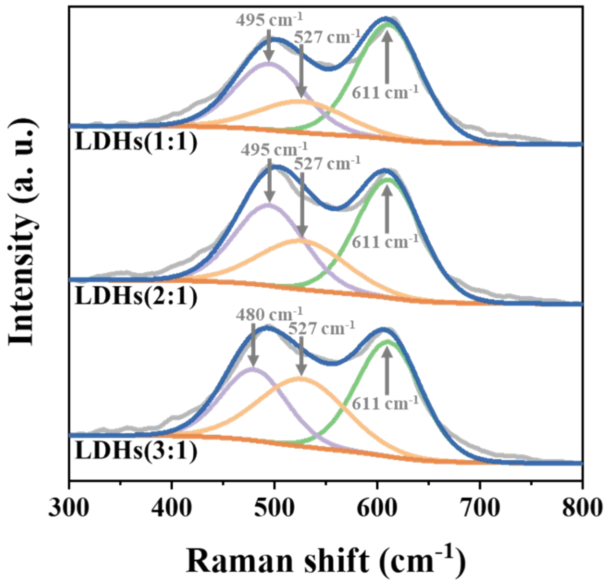

Figure S3. Raman spectra of NiCoMn-LDHs with different ratios.

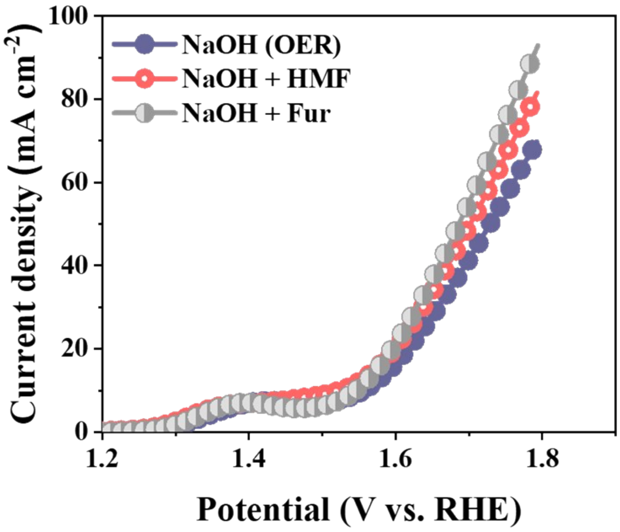

Figure S4. LSV curves of NF in different electrolytes.

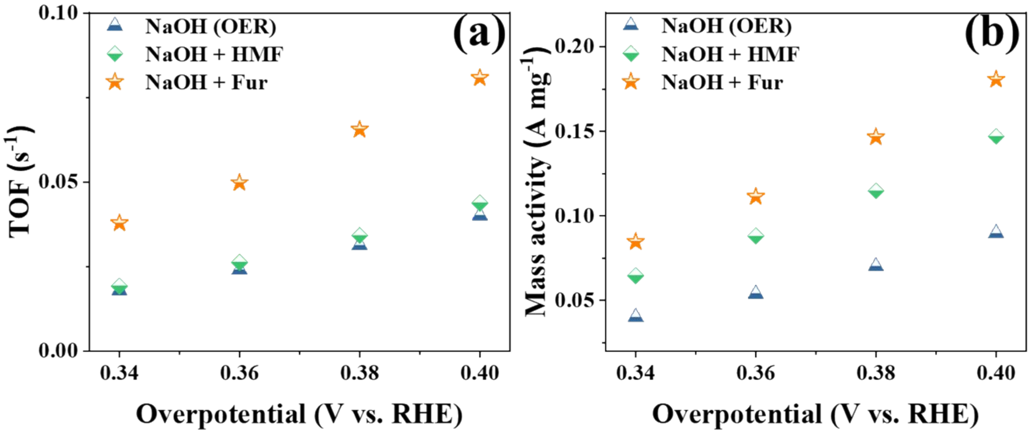

Figure S5. (a) TOF plots and (b) mass activity of NiCoMn(2:1)-LDHs/NF in different electrolytes at different overpotentials.

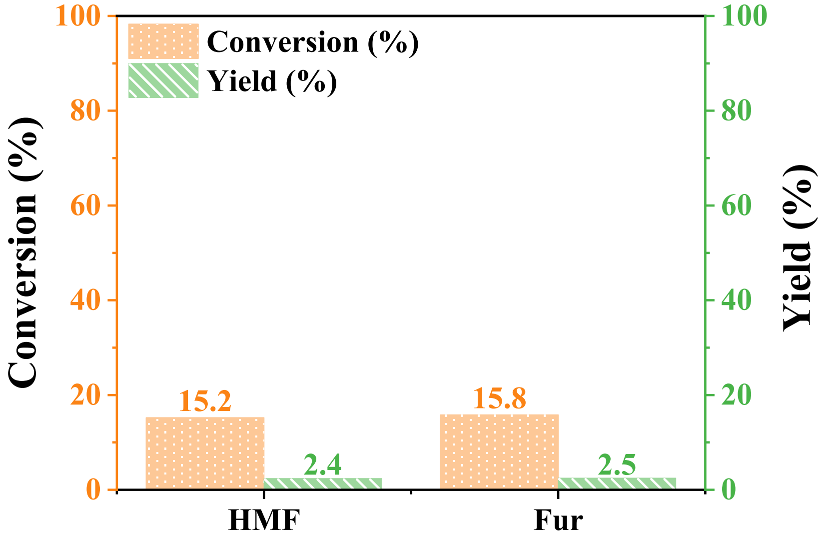

Figure S6. The conversion of 1 mM HMF and furfural and the yield of FDCA and FurAc at temperature of 35 ^{o}C by using pure NF.

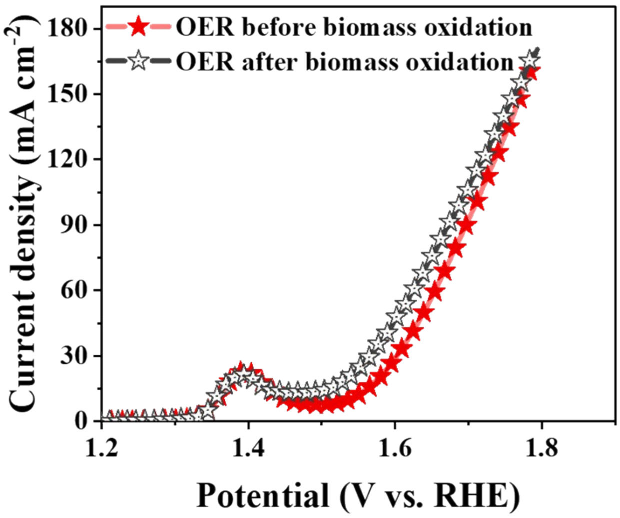

Figure S7. The cyclic stability test in 1 M NaOH at a sweep rate of 10 mV s^{-1} of NiCoMn(2:1)-LDHs/NF in a four-necked round flask.

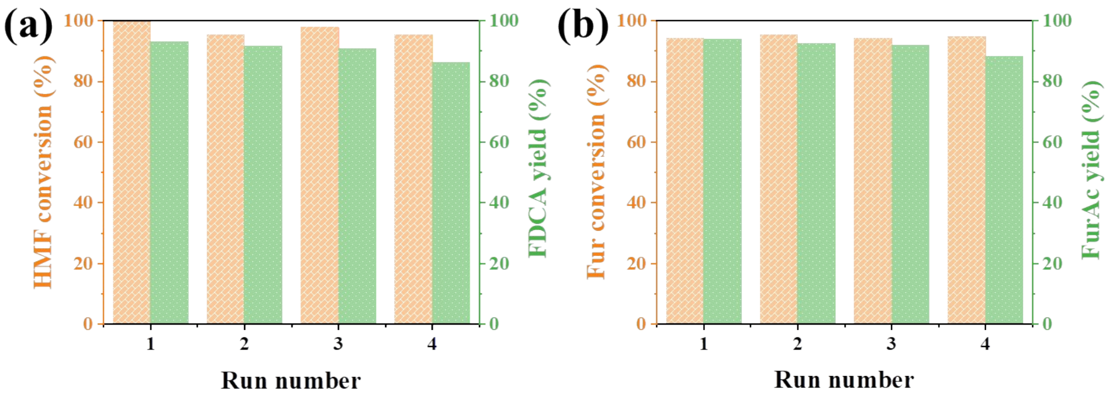

Figure S8. Consecutive use of NiCoMn(2:1)-LDHs/NF under 35 °C in 1 M NaOH containing 1 mM HMF in 150 min.

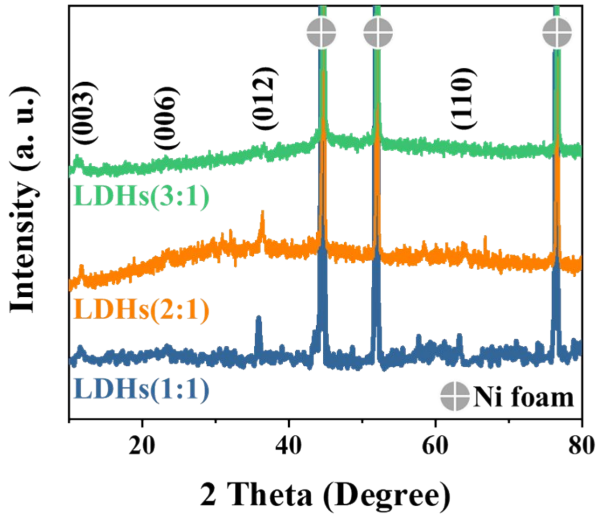

Figure S9. XRD patterns of NiCoMn-LDHs/NF with different ratios after oxidation reaction.

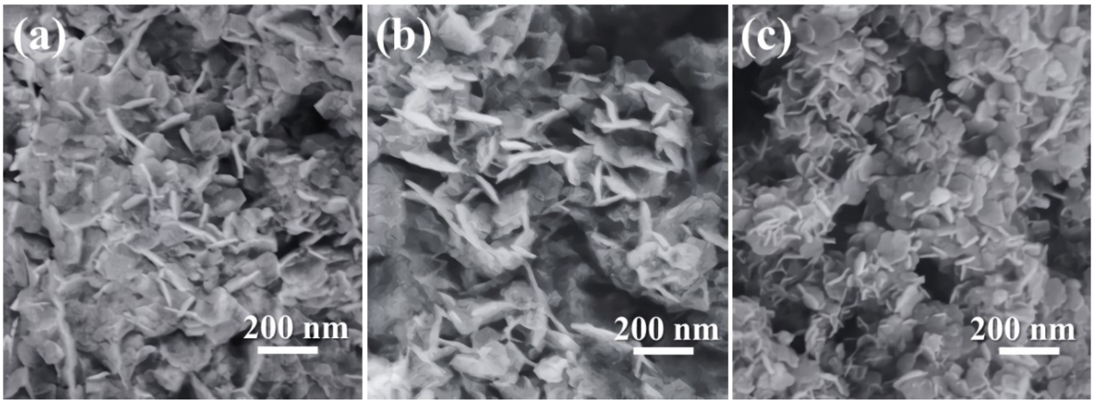

Figure S10. SEM images of NiCoMn(2:1)-LDHs/NF. (a) Before oxidation. (b) After HMF oxidation. (c) After furfural oxidation.

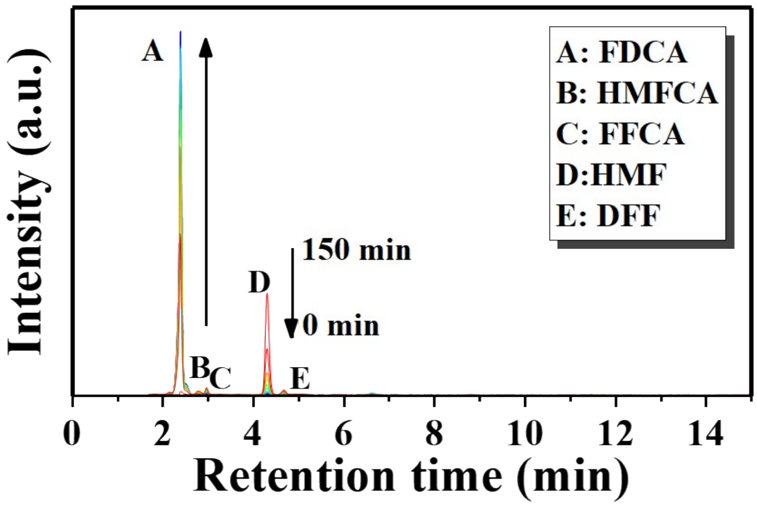

Figure S11. HPLC spectrum of the oxidation of 1 mM HMF at 35 ^{o}C in 150 min.

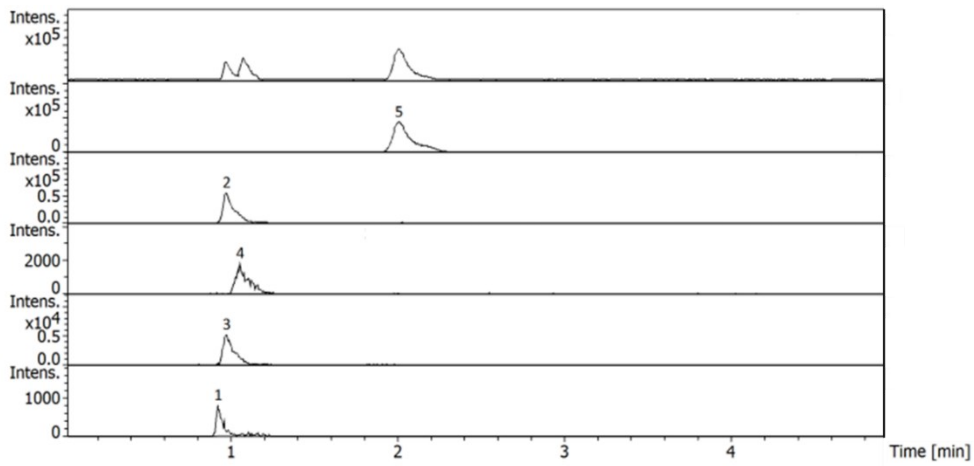

#	RT [min]	Area	I	Trace
1	0.9	1982.5	810	EIC C6H4O5 [M+H]+ 157.0131±0.002 All MS
2	1.0	259119.1	56225	EIC C6H4O3 [M+H]+ 125.0233±0.002 All MS
3	1.0	25086.1	5364	EIC C6H6O4 [M+H]+ 143.0339±0.002 All MS
4	1.1	9352.7	1823	EIC C6H4O4 [M+H]+ 141.0182±0.002 All MS
5	2.0	702191.7	90128	EIC C6H6O3 [M+H]+ 127.0390±0.002 All MS

Figure S12. LC-MS spectra of intermediate products during the oxidation of HMF.

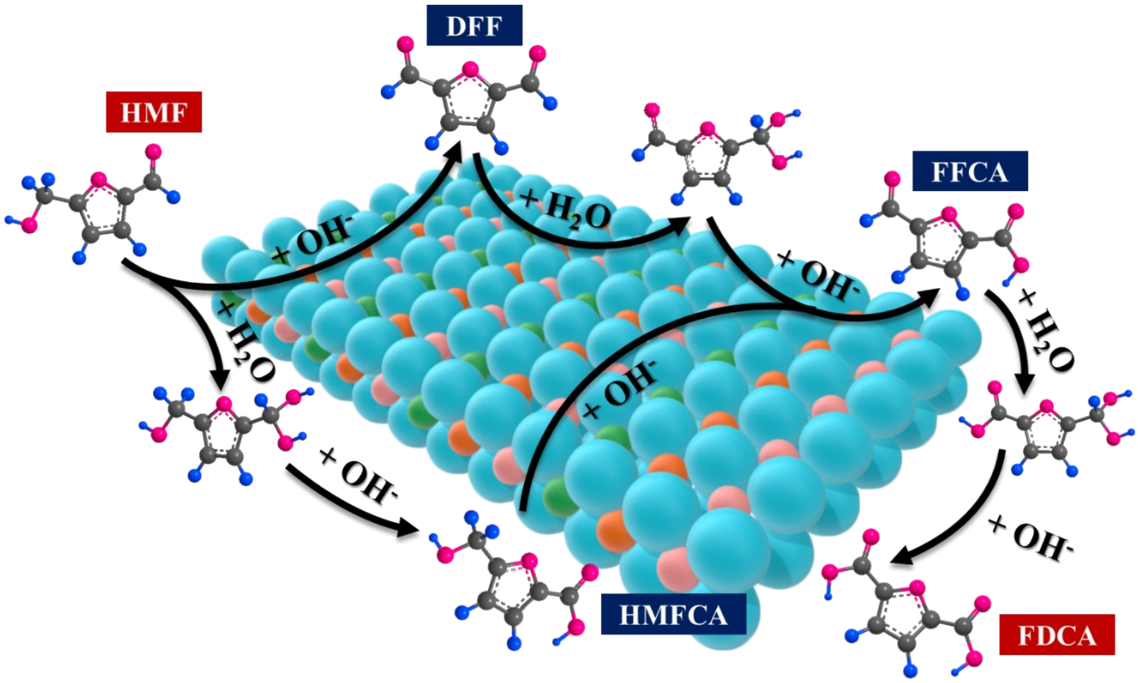

Figure S13. The possible oxidation pathways of HMF to FDCA on NiCoMn-LDHs/NF.

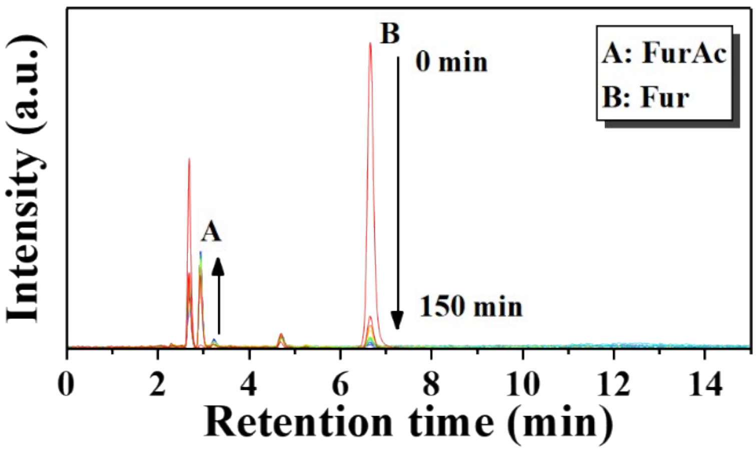

Figure S14. HPLC spectrum of the oxidation of 1 mM furfural at 35 ^{o}C in 150 min.

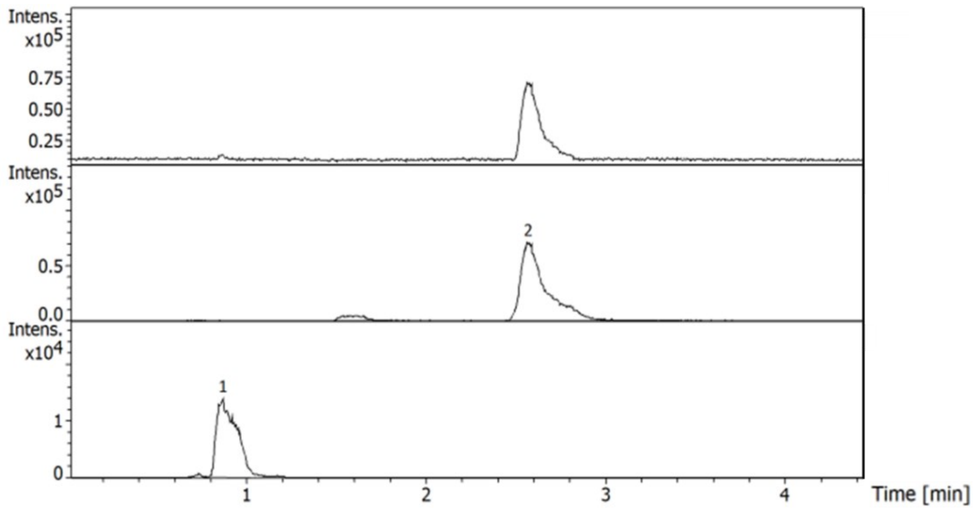

#	RT [min]	Area	I	Trace
1	0.9	107553	14146	EIC C5H4O3 [M+H]+ 113.0233±0.005 All MS
2	2.6	702598	71878	EIC C5H4O2 [M+H]+ 97.0284±0.005 All MS

Figure S15. LC-MS spectra of products during the oxidation of furfural.

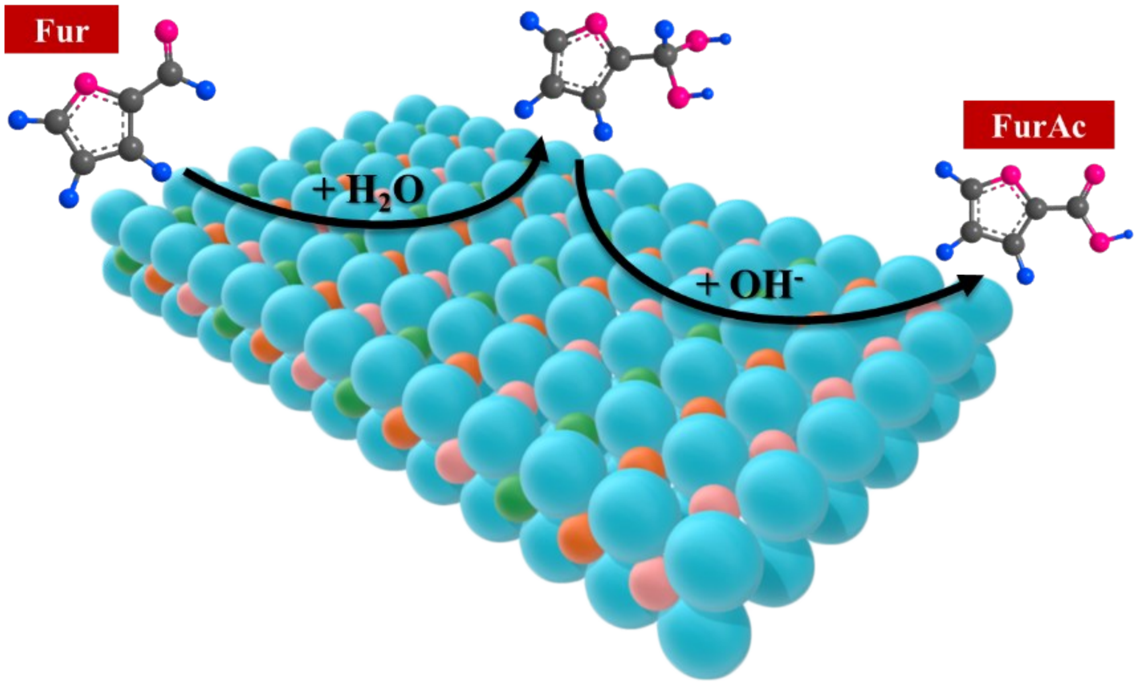

Figure S16. The possible oxidation pathways of furfural to FurAc on NiCoMn-LDHs/NF.

References

1. W.-J. Liu, L. Dang, Z. Xu, H.-Q. Yu, S. Jin and G. W. Huber, *ACS Catal.*, 2018, **8**, 5533-5541.

2. M. Zhang, Y. Liu, B. Liu, Z. Chen, H. Xu and K. Yan, *ACS Catal.*, 2020, **10**, 5179-5189.

3. B. J. Taitt, D.-H. Nam and K.-S. Choi, *ACS Catal.*, 2019, **9**, 660-670.

4. M. J. Kang, H. Park, J. Jegal, S. Y. Hwang, Y. S. Kang and H. G. Cha, *Appl. Catal. B-Environ.*, 2019, **242**, 85-91.

5. Z. Zhou, C. Chen, M. Gao, B. Xia and J. Zhang, *Green Chem.*, 2019, **21**, 6699-6706.

6. G. Chamoulaud, D. Floner, C. Moinet, C. Lamy and E. M. Belgsir, *Electrochim. Acta*, 2001, **46**, 2757-2760.

7. P. Parpot, A. P. Bettencourt, G. Chamoulaud, K. B. Kokoh and E. M. Belgsir, *Electrochim. Acta*, 2004, **49**, 397-403.